Available online at www.sciencedirect.com
SCIENCE DIRECT®
Agriculture, Ecosystems and Environment 107 (2005) 21–35
Agriculture Ecosystems & Environment
www.elsevier.com/locate/agee

Alternate satellite models for estimation of sugar beet residue nitrogen credit

Ofer Beeri[a,*], Rebecca Phillips[a], Pete Carson[b], Mark Liebig[c]

[a]*Upper Midwest Aerospace Consortium, University of North Dakota, Tulane Drive, P.O. Box 9007, Grand Forks, ND 58202-9007, USA*
[b]*Carson Farms, 7953 Highway 81, St. Thomas, ND 58276, USA*
[c]*USDA-ARS, Northern Great Plains Research Laboratory, P.O. Box 459, Mandan, ND 58554, USA*

Received 6 April 2004; received in revised form 30 September 2004; accepted 21 October 2004

Abstract

Satellite assessment of aboveground plant residue mass and quality is essential for agro-ecosystem management of organic nitrogen (N) because growers credit a portion of residue N towards crop requirements the following spring. Precision agriculture managers are calling for advanced satellite models to map field-scale residue mass and quality. Remote sensing has proven useful for assessing the concentration of foliar biochemicals under controlled laboratory conditions, but field-scale satellite model validation for quantitative, landscape-scale N assessment is needed. We addressed this problem by building ground-truth models for sugar beet N-credit and testing these models with alternate satellite sensor imagery. We recorded spectral reflectance and measured leaf carbon (C) and N in situ at leaf and canopy levels near the end of the growing season using 1 nm bandwidth spectroradiometer. We performed univariate correlation analyses between spectral reflectance and the variables N, C:N ratio and biomass to determine spectral signature models for leaf quality and spectral signature models for plant biomass. The 1 nm hyperspectral data were convolved to fit Landsat 5, SPOT 5, Quick-Bird 2, and Ikonos 2 multi-spectral satellite bands and models created using stepwise linear regression. Biomass formulae for each sensor were applied to satellite imagery acquired at peak season, while leaf quality formulae were applied to imagery acquired just prior to harvest. August sugar beet fields in the St. Thomas, ND vicinity were identified and aboveground biomass mapped with 10–20% error, depending upon the sensor. Sugar beet leaf N was similar for all sites and varieties tested (31 mg g^{-1} dw), so biomass primarily influenced N-credit estimates. Measured C:N ratio variability was identified and mapped to delineate areas where C:N ratio was outside the normal distribution. The general model for each sensor maps N-credit per unit area and delineates aberrant, low leaf quality areas as zones with high C:N ratio. In summary, we provide separate spectral models for N-credit and leaf quality applicable to available multi-spectral sensors for precision sugar beet N management.

Keywords: Hyperspectral; Multi-spectral; Sugar beet *Beta vulgaris* (L.); Satellite comparison; C:N ratio; N-credit

* Corresponding author. Tel.: +1 701 777 6095; fax: +1 701 777 2940.
E-mail address: beeri@umac.org (O. Beeri).

0167-8809/$ – see front matter © 2004 Elsevier B.V. All rights reserved.
doi:10.1016/j.agee.2004.10.030

1. Introduction

Fertilization management is essential for balancing productivity and profits in agro-ecosystems, although environmental impacts associated with N fertilization is an emerging area of concern (Nosengo, 2003). An increasing body of scientific evidence indicates that excessive N fertilization negatively influences water quality, air quality and ecosystem biodiversity (Vitousek, 1997). Consequently, scientific and political communities are calling for agro-ecosystem managers to explore technological tools to reduce nitrate in groundwater, atmospheric nitric acid, ammonium deposition, and emissions of greenhouse gases (Nosengo, 2003).

One way growers can reduce N inputs is by estimating organic N remaining in crop residues to offset or reduce synthetic N application, a task which could be advanced with satellite data products (Whitmore and Groot, 1997). Sugar beet (*Beta vulgaris* L.) leaf tops are particularly N-rich and remain in soils following harvest (Moraghan and Smith, 1996), with reportedly 47% of fertilizer N inputs stored in aboveground leaf material (Vos and van der Putten, 2000). Most of this N "sink" is in leaf (rather than stem) biomass, contributing from 100 to 450 kg ha^{-1} that is commonly ploughed back into soil in autumn (Vos and van der Putten, 2000; Franzen et al., 2001). In 2002, over 200,000 ha of sugar beets were cultivated in the Red River Valley of the North Ecoregion, USA (Fig. 1).

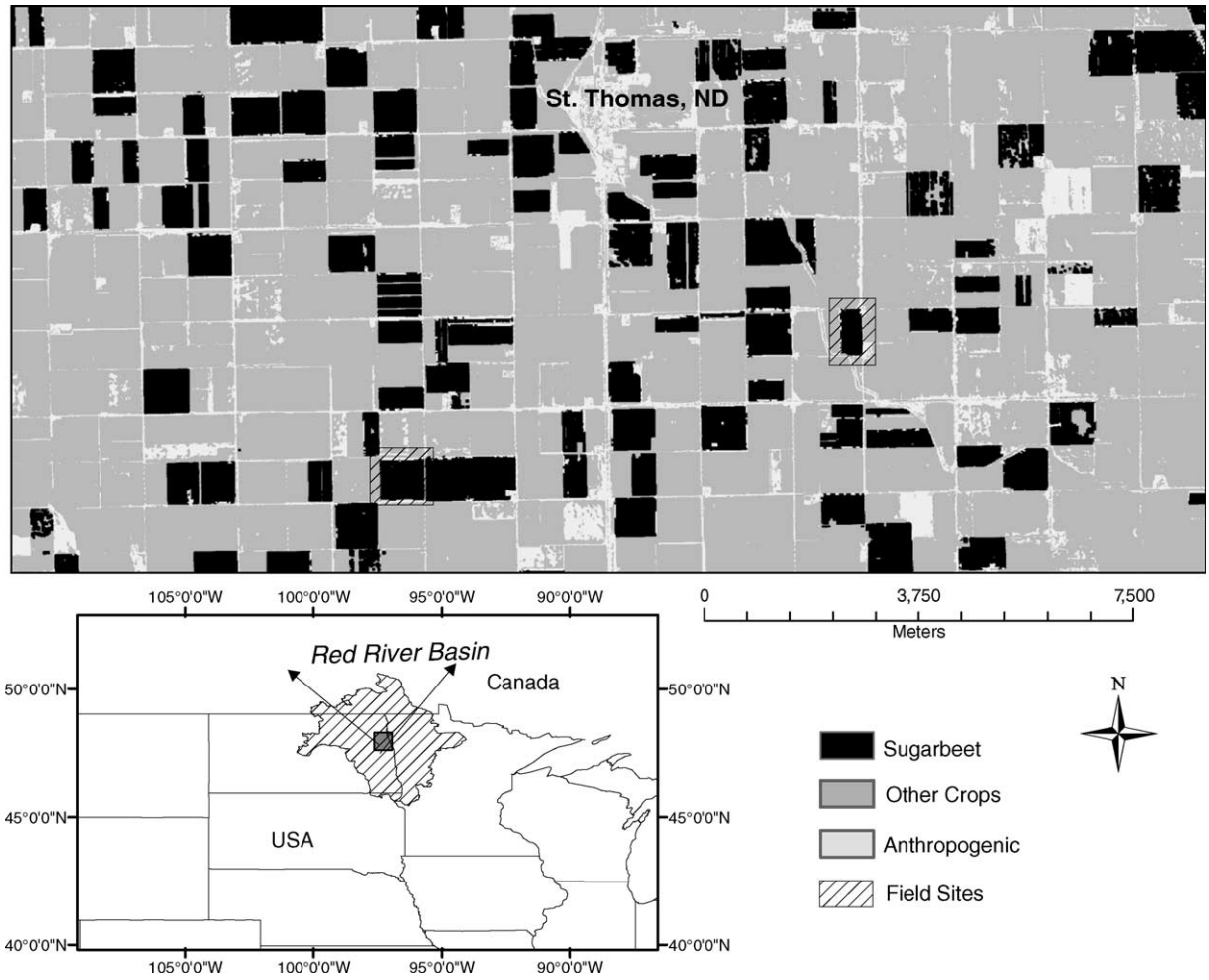

Fig. 1. Study area inside the Red River Basin, near St. Thomas, North Dakota.

If the N-credit for this region were 100 kg ha^{-1}, N fertilization input could have been reduced by 20,000 metric tons in 2003. Actual N-credit, however, is highly variable (depending upon crop growth parameters) so it must be estimated within and between fields each year (Abshahi et al., 1984; Vos and van der Putten, 2000; Franzen et al., 2001). Precision agriculture managers, therefore, are calling for synoptic detection of N in plant residues, so that excessive fertilization may be avoided (Sims et al., 2002). Satellite data models present a clear option for improved N management through integration of spatial and temporal crop information over large areas.

The N-credit assigned to a field or field-section can be defined as the amount of N in plant leaf residue (Moraghan and Smith, 1996), calculated as the product of leaf biomass and N content (Eq. (1)):

$$\text{residue N-credit} = [B_{\text{fresh}} \times L_{\text{fraction}}] \times \left[\frac{(\text{leaf N}/1000)}{(1 + M_{\text{fraction}})}\right] \quad (1)$$

where B is aboveground biomass (kg ha^{-1}), L the fraction of aboveground leaf biomass without stems, leaf N is amount of nitrogen determined analytically in dry leaf material [mg g^{-1} dry weight (dw)], and M is leaf water content. Aboveground biomass is often spectrally estimated according to indices such as the normalized difference vegetation index [NDVI: $(R_{\text{nir}} - R_{\text{red}})/(R_{\text{nir}} + R_{\text{red}})$] and the green normalized difference vegetation index [GNDVI: $(R_{\text{nir}} - R_{\text{green}})/(R_{\text{nir}} + R_{\text{green}})$], where R is the reflectance at a specific bandwidth. These indices are especially useful for heterogeneous systems in nature. For homogenous sugar beet agro-ecosystems, spectral biomass models may be more accurate than NDVI (Bouman, 1992; Clevers, 1997; Guerif and Duke, 2000; Reeves et al., 2001). Although indices are valuable tools with demonstrated applications, they by definition prevent multi-spectral separation of biomass from leaf quality. For N-credit estimation, biomass and N are independent, so we developed individual spectral models for each variable and satellite sensor.

Remote sensing aerial and ground level platforms can be modeled to detect specific leaf N content (Boegh et al., 2002; Mutanga et al., 2004), but multi-spectral satellite imagery applications are lacking (Moran et al., 1997). Boegh et al. found that aerial data in the green and far-red bands were correlated with leaf N for multiple crops. Mutanga et al. found that selected, 1 nm width wavelengths (417, 438 and 2125 nm) collected at ground level were correlated with leaf N in slightly senescent natural grasslands of diverse vegetation (Mutanga et al., 2004). However, it is not known how well multi-spectral satellite platforms (for which spectral bandwidths are often several hundred nm) can delineate leaf N. Research indicates that leaf N carries a unique spectral signature, yet multi-spectral satellite platform applications should be demonstrated (Jacquemoud et al., 1995; Kokaly and Clark, 1999).

Another factor influencing N-credit is leaf quality. The ratio of C:N is suggestive of leaf quality and a common reference among plant ecologists. When C:N ratio is high, leaf material is not easily mineralized, so high C:N ratio leaf material is considered low quality. The actual amount of N stored in leaf tops that is mineralized and mobilized in spring depends upon the C:N ratio of the residue (Whitmore and Groot, 1997). Therefore, C:N ratio indirectly affects N-credit by controlling N availability.

Since our goal was to provide large scale information applicable to precision N management in 'real world' agro-ecosystems, we needed to extend beyond controlled laboratory conditions and collect ground data from sugar beet fields in production, as suggested by Moran et al. (1997). Consequently, we studied sugar beet fields managed by local growers to build ground-truth models with spectral and chemical analyses. We applied these models to alternate multi-spectral satellite sensors and evaluated the utility of these results in an agribusiness environment. We enlisted the cooperation of two established sugar beet land managers during the summer of 2003 in the Red River Valley, North Dakota, one of the two largest sugar beet production regions in the USA (Leff et al., 2004).

2. Methods

2.1. Overview

We investigated two sugar beet fields in the Red River Valley near St. Thomas ND (97°27′W; 48°37′N) seeded during the same week in April 2003 (Fig. 1).

Sites were <5 km away from each other and similar with regard to climate, historical land-use and soil series (Glyndon silt loam; Coarse-silty frigid Aeric Calciaquoll). The west site (PC789) was a 28 ha field where leaf C ($\mu g\ g^{-1}$), leaf N ($\mu g\ g^{-1}$), plant N ($g\ plant^{-1}$), and fresh leaf biomass ($kg\ ha^{-1}$) were measured and sugar beet leaf spectral signatures recorded. The east site (AT05) was a 30 ha field where fresh leaf biomass ($kg\ ha^{-1}$) was measured and canopy spectra recorded. We evaluated field measurements from both sites to build and test N-credit satellite models for agricultural managers. These were developed by achieving the following objectives: (1) determine spectral regions most highly correlated with leaf N, C:N ratio and biomass, (2) aggregate hyperspectral ground data to fit multi-spectral satellite sensors Landsat 5, SPOT 5, Ikonos 2, and Quick-Bird 2, (3) derive formulae from the aggregated spectra to estimate leaf N, C:N ratio and canopy biomass, (4) assess accuracy for each satellite sensor model, and (5) map N-credit and leaf quality (C:N ratio) for the St. Thomas, ND landscape. Methods required for this interdisciplinary study are outlined according to field site surveyed.

2.2. Field PC789 ground data

Field PC789 was selected based on soil homogeneity, as determined by random soil tests for nitrogen, phosphorous, potassium and micronutrients (Simplot, Inc., Grafton, ND).[1] PC789 was seeded with four sugar beet varieties in a 4 × 2 randomized block design: American Crystal Sugar 999 (ACS 999), Beta 6600, Holly 811, and Vanderhoff 556 (VDH 556). Two random points within replicate strips were selected using 3 m resolution data by ERDAS Imagine (Version 8.6) random generator. Plant samples at each point were collected on September 15, 2003, approximately 2 weeks before harvest. Each point was located with a Trimble GPS and beacon for sub-meter positional accuracy. At each point, one entire beet plant was cut to ground level, and leaf material was separated into three leaf size groups: small (5–10 cm wide), medium (10–15 cm wide) and large (>15 cm wide). Leaf spectra were recorded for each leaf size group (48 total) using a hand-held spectroradiometer (ASD Instruments, Boulder, CO). Reflectances were recorded in 1 nm bands between 350 and 2500 nm from a height of 0.25 m above the leaf. The spectroradiometer was calibrated between each leaf size group at each location. Five spectral measurements were recorded for each of the 48 samples to obtain an average.

Aboveground biomass ($g\ m^{-2}$) was collected near the original 16 sites on October 3, 2003. Beet tops within a $1\ m^2$ plot were clipped to ground level, bagged and weighed. PC 789 biomass data were utilized for evaluating formulae created using the AT05 field site ground data.

Correlation analyses were performed for hyperspectral ground data to determine the spectral region most highly correlated with leaf N by leaf size group (Fig. 2). Hyperspectral data collected at ground level were then convolved to multi-spectral bands according to sensor-specific radiometric parameters (Jacquemoud et al., 1995) for Ikonos 2, SPOT 5, Quick-Bird 2, and Landsat 5 (Table 1). These convolutions simulate satellite-borne sensor response and facilitate comparisons among sensors and sensor platforms (Table 2). We separately analyzed convolved bands that correlated with leaf N and C:N ratio to determine if those bands varied significantly with leaf size using the SAS Proc GLM analysis of variance and distinguished groups according to Tukey's least significant difference test (SAS Institute, Cary, NC).

Leaf N ($mg\ g^{-1}$ dw) and C:N ratio were statistically analyzed to test for differences among varieties and leaf size categories using the SAS Proc GLM analysis of variance and significantly different groups determined according to Tukey's least significant difference test. In addition, total N per plant was calculated by totaling weighted means for each leaf size category. Plant N ($kg\ ha^{-1}$) was multiplied by the number of plants harvested as an alternative method for aboveground N estimation.

Correlation and stepwise regression procedures between leaf N ($mg\ g^{-1}$ dw) and convolved spectra, and C:N ratio and convolved spectra were utilized for creating sensor-specific formulae. N and C:N ratio formulae results were mapped using imagery acquired within 10 days of sample collection.

[1] Mention of commercial products and organizations in this article is to provide specific information only. It does not constitute endorsement by UMAC, UND, or USDA-ARS over other products and organizations not mentioned.

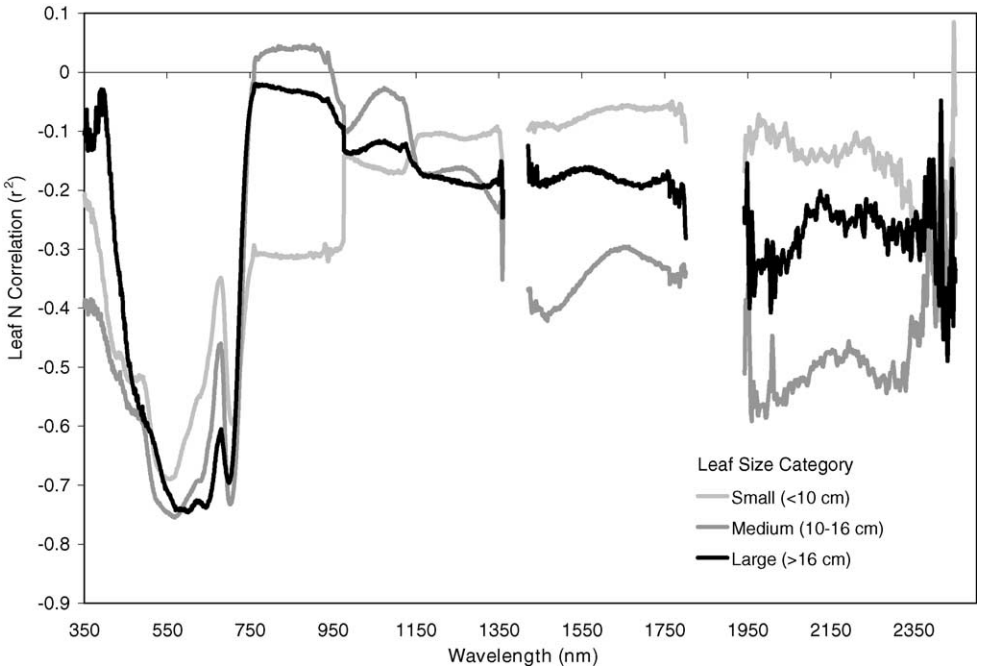

Fig. 2. Correlation between hyperspectral ground data and leaf N for each leaf size group ($n = 15$) recorded September 15, 2003 in field PC789.

Table 1
Satellite imagery acquired in 2003, including satellite references specifications for spectral response curves

Sensor name	Path-row	Date	Sensor reference
Landsat 5	031–026	August 16	http://ltpwww.gsfc.nasa.gov/ias/handbook/handbook_htmls/chapter8/html
SPOT 5	573–251	July 18	http://www.spotimage.fr/html/_167_224_229_.php
SPOT 5	573–252	August 13	http://www.spotimage.fr/html/_167_224_229_.php
SPOT 5	573–252	September 23	http://www.spotimage.fr/html/_167_224_229_.php
Ikonos 2	Custom	August 8	http://www.spaceimaging.com/products/ikonos/spectral.htm
Ikonos 2	Custom	September 7	http://www.spaceimaging.com/products/ikonos/spectral.htm
Quick-Bird 2	Custom	July 28	Dr. Jack, F. Parris, New Products R&D Group, Digital Globe, Inc.

2.3. Field AT05 ground data

AT05 was seeded with one sugar beet variety, American Crystal Sugar 817 (ACS 817), in April 2003. A north to south productivity gradient existed for this field, so it was divided into three equal sections. Three locations within each section were randomly selected for spectral and biomass sampling. At each location, four plots (0.2 m × 3 m) ~10 m apart were staked for repeated spectral measurements and biomass determination. Spectral data were recorded at these points on August 16, September 4 and September 15 using the hand-held spectro-radiometer. Ten spectral readings were recorded at

Table 2
Average leaf N (mg g^{-1} dry weight) ±1 standard deviation measured vs. model estimates by size for all varieties

Leaf size	Leaf N measured	Landsat 5		Quick-Bird 2		SPOT 5		Ikonos 2	
		Estimated N	R^2	Estimated N	R^2	Estimated N	R^2	Estimated N	R^2
Small	40.4 ± 9.9	40.8 ± 4.3	0.55	40.7 ± 4.4	0.55	37.5 ± 5.7	0.36	40.8 ± 4.4	0.55
Medium	37.2 ± 8.0	33.1 ± 7.1	0.55	33.3 ± 7.0	0.55	32.9 ± 6.4	0.36	33.2 ± 7.0	0.55
Large	27.2 ± 6.6	30.3 ± 7.3	0.55	30.0 ± 7.4	0.55	34.3 ± 5.2	0.36	30.1 ± 7.3	0.55

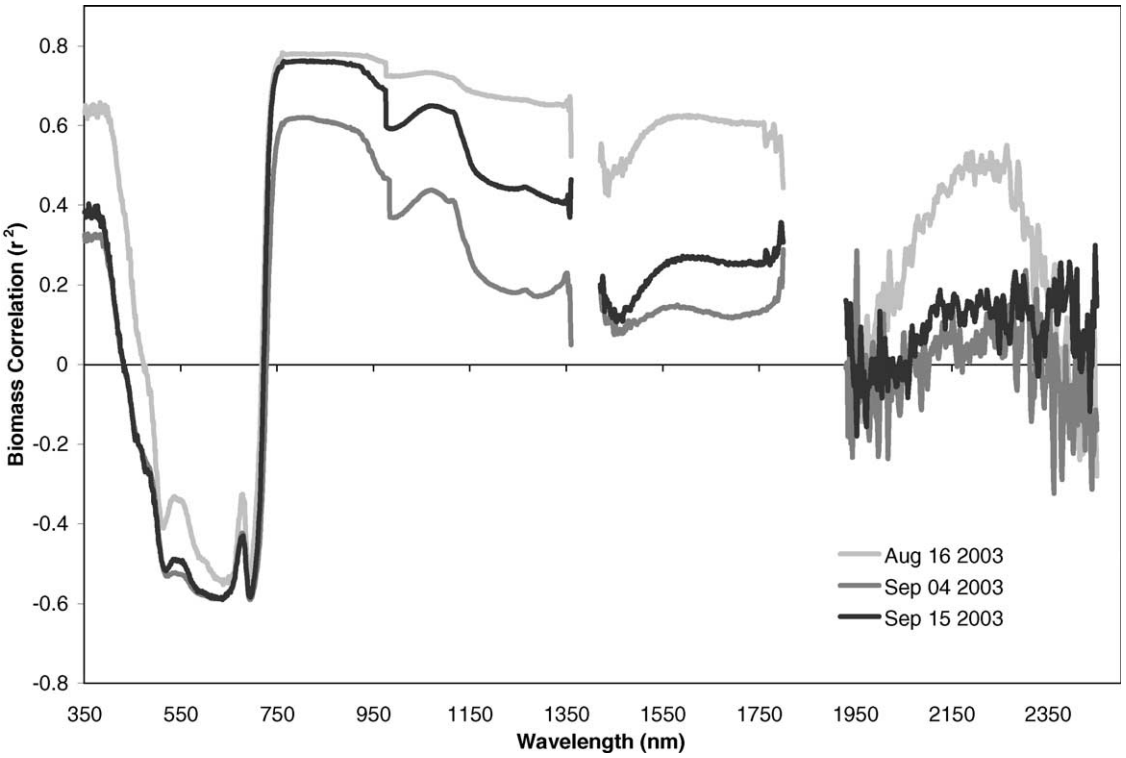

Fig. 3. Correlation between hyperspectral ground data collected on three dates and aboveground biomass ($n = 36$) recorded in field AT05.

the canopy level (1.5 m above leaf tops) to obtain the average per plot for each date.

Aboveground plant material for all 36 plots was clipped to ground level and weighed on September 23. Correlation and stepwise regressions were performed (as in field PC789) to create sensor-specific biomass models (Fig. 3). Further, indices commonly used to estimate biomass (NDVI, GNDVI) were also tested with correlation analyses. Spectral biomass estimates were mapped using Quick-Bird 2, Landsat 5, SPOT 5, and Ikonos 2 satellite images and validated with 24 ground points.

2.4. Satellite data processing

Images from four different satellite sensors were acquired (Table 1), calibrated and tested using ground based spectra. Digital numbers were corrected to ground reflectance with the following (Eq. (2)):

$$R_x = \frac{(\pi^* d^{2*}(\text{gain}_x^*(\text{DN}_x - \text{min}_x)))}{(\text{E-SUN}_x^* \sin(\theta))} \quad (2)$$

where R is the ground reflectance for each band ($_x$), d the Earth–Sun distance in astronomical units for the image date, gain is the band specific rescaling factor, DN represents digital number in the raw image, min the lower DN in the specific band (Chavez, 1996), E-SUN the mean solar exoatmospheric irradiance, and θ the sun elevation angle (Huang et al., 2002; NASA, 2003).

Classification for the research area was performed using SPOT and Landsat imagery with decision tree landscape analysis. Five major classes were identified for N-credit mapping: water, anthropogenic, uncultivated vegetation, sugar beet crops, and other crops. Classification accuracy was 90%, with an overall Kappa Statistic of 0.8638.

2.5. N-credit satellite model

Spectral models derived for satellite sensor application were evaluated for accuracy by comparison with ground-truth data. Sensor model errors for N-credit and leaf quality were compared by calculat-

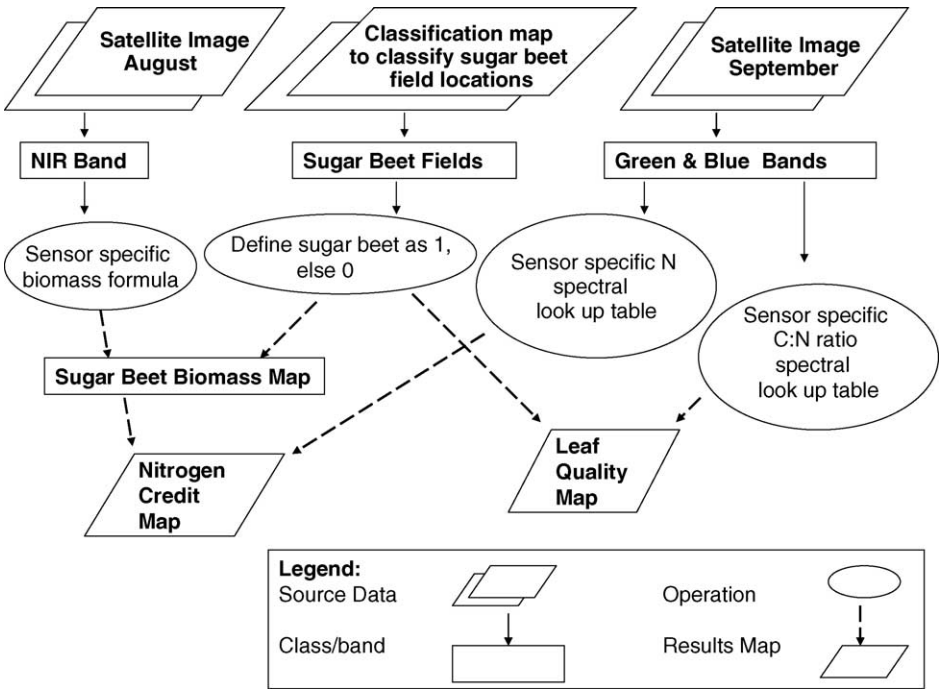

Fig. 4. Schematic illustration of N-credit model using satellite formulae estimates for biomass, N and C:N ratio.

ing the deviations of predicted values from observed values, summing up the measurements, and then taking the square root of the sum. The result is the root mean square error (RMSE) or the standard deviation of the residuals, which depicts the error associated with each model prediction compared to observed values. The final N-credit map depicts spatial information for canopy N content and biomass, while the final leaf quality map denotes areas of high, medium or low C:N ratio (Fig. 4).

3. Results

3.1. Plant leaf and canopy spectral ground data

3.1.1. Leaf nitrogen and C:N ratio

Leaf N was similar among the four sugarbeet varieties, but large leaf N was 30% lower overall than for small and medium leaf N (Table 2). Sugar beet spectral signatures were most highly correlated with leaf N in the 490–600 nm, blue-green range (Fig. 2). A good correlation was also evident in the narrow wavelength band between 690 and 720 nm. Since multi-spectral satellite data for this region were not available, these data were not included in subsequent analyses. Results of the stepwise regressions indicated that the convolved green and blue bands significantly contributed to sensor-specific leaf N models. Spectral estimates for leaf N indicated that N was similar among varieties but varied significantly among leaf sizes for Landsat 5, Quick-Bird 2 and Ikonos 2 sensor bands. Overall, values predicted using Ikonos 2, Quick-Bird 2 and Landsat 5 sensors were between 13 and 22% of actual leaf N for all leaf sizes (see RMSE Table 3). The SPOT 5 sensor lacks blue spectra, so the SPOT 5 did not perform as well as the others for leaf N. Tukey's least significant difference test for Landsat 5, Quick-Bird 2 and Ikonos 2 spectral estimates indicated that small leaf N was significantly higher than large leaf N, which is consistent with the leaf chemical data ($P < 0.05$). However, the spectral models did not differentiate medium from large leaf N. Satellite estimates did not delineate leaf N content between 27 and 37 mg g^{-1} dw.

The relationship between leaf size and C:N ratio was similar to the relationship between leaf size and

Table 3
Spectral formula and formula evaluation (root mean square error, RMSE) using data acquired for each sensor

Sensor	Acquired	C:N ratio formula[a]	RMSE	Leaf N (%) formula	RMSE	Biomass formula	RMSE
Ikonos 2							
Nitrogen	September 7	$Y = 5.63 - (213.54 \times B) + (165.61 \times G)$		$Y = 5.21 + (67.38 \times B) - (49.01 \times G)$		If NIR > 0.516; $Y = 152923 \times NIR - 38995$	
Biomass	August 8	ACS 999	2.63	Small	6.10		8104
		Beta 6600	1.52	Medium	5.00		
		Holly 811	1.77	Large	4.70		
		VDH 556	1.35				
SPOT 5							
Nitrogen	September 23	$Y = 2.94 + (85.13 \times G)$		$Y = 6.06 - (23.40 \times G)$		If NIR > 0.520; $Y = 155128 \times NIR - 40478$	
Biomass	August 13	ACS 999	2.93	Small	6.70		8514
		Beta 6600	1.59	Medium	5.70		
		Holly 811	2.08	Large	7.70		
		VDH 556	2.41				
Quick-Bird 2							
Nitrogen	July 28	$5.63 - (215.70 \times B) + (167.98 \times G)$		$5.22 + (67.26 \times B) - (49.34 \times G)$		If NIR > 0.517; $Y = 153686 \times NIR - 39436$	
Biomass	July 28	ACS 999	2.62	Small	6.10		7937
		Beta 6600	1.53	Medium	5.00		
		Holly 811	1.76	Large	4.70		
		VDH 556	1.36				
Landsat 5							
Nitrogen	August 16	$6.04 - (229.08 \times B) + (171.16 \times G)$		$5.08 + (72.89 \times B) - (51.14 \times G)$		If NIR > 0.520; $Y = 155492 \times NIR - 40591$	
Biomass	August 16	ACS 999	2.59	Small	5.80		8790
		Beta 6600	1.42	Medium	5.10		
		Holly 811	3.64	Large	4.70		
		VDH 556	1.27				

[a] B and G represent the blue and green bands, respectively, and NIR represents the near infra-red band.

Table 4
Average leaf C:N ratio ±1 standard deviation measured vs. model estimates by variety for all leaf sizes

Variety	C:N ratio measured	Landsat 5		SPOT 5		Quick-Bird 2		Ikonos 2	
		Estimated C:N	R^2	Estimated C:N	R^2	Estimated C:N	R^2	Estimated C:N	R^2
ACS	14.38 ± 4.8	13.71 ± 3.45	0.51	13.73 ± 2.75	0.36	13.84 ± 3.41	0.51	13.80 ± 3.40	0.51
Beta	11.05 ± 2.2	11.72 ± 1.59	0.51	11.12 ± 1.25	0.36	11.72 ± 1.65	0.51	11.70 ± 1.65	0.51
Holly	11.23 ± 2.4	11.97 ± 2.99	0.51	12.49 ± 1.51	0.36	11.99 ± 3.10	0.51	11.98 ± 3.07	0.51
VDH	11.79 ± 3.1	11.82 ± 2.14	0.51	11.76 ± 1.97	0.36	11.70 ± 2.05	0.51	11.71 ± 2.08	0.51

N. Small and medium leaves were highest in leaf quality, with C:N ratios of 10.9 and 11.2, respectively. Average large leaf C:N ratio was 14.6, indicating that leaf quality is significantly lower in the larger leaves ($P < 0.05$). Leaf C:N ratio also varied with variety, with ACS 999 significantly greater than Beta 6600 for all leaf sizes (Table 4). Leaf C:N ratio spectral formulae, derived using stepwise regression for each sensor, also utilized convolved green and blue bands. Formulae estimates using convolved data varied with sensor, but sensor prediction error was between 13 and 30% of actual leaf C:N for all varieties (see RMSE Table 3). We did not find significant differences between actual and spectral leaf C:N ratio estimates using comparison *t*-tests, suggesting the potential for satellite detection of leaf canopy C:N.

3.1.2. Biomass

Sugar beet spectral signatures in the near infra-red (NIR) region (760–925 nm) were most highly correlated with biomass for all dates at the canopy level (Fig. 3). This NIR plateau is common among vegetation spectra, and the 165 nm width for this region is well suited for broadband multi-spectral sensor applications. NDVI and GNDVI indices were also tested, and results were similar to using the NIR only. Leaf N and C:N ratio could not be delineated in the NIR (Fig. 2), and this allowed us to independently evaluate leaf quality from biomass models.

Biomass estimation at peak season in August was required to avoid errors introduced by early September pre-harvest and leaf senescence. Also, the correlation between spectral signature and biomass was greatest at peak season when plants were highly productive and at full cover (Fig. 3). Spectral ground data, beet phenology, and removal of material at pre-harvest suggested optimum image acquisition during August.

Average biomass for the high productivity section of AT05 (50,000 kg ha^{-1}) was significantly greater ($P < 0.01$) than biomass for the low productivity section (31,000 kg ha^{-1}), while biomass for the center field section (38,000 kg ha^{-1}) was intermediate. Convolved NIR spectral values were also ∼20% greater for high productivity sections, compared to low, with a region of delineation near 0.5 reflectance, depending upon sensor. Significant differences in the low productivity sites precluded combining these data with the more typical, productive sites. Consequently, equations formulated were according to intermediate and high production field sites using the NIR region >0.5 reflectance (Tables 3 and 5). Although the stepwise regression suggested that both the NIR and

Table 5
Average sugar beet biomass model estimates (kg ha^{-1}) ± 1 standard deviation by sensor and image acquisition date

Sensor	Imagery acquired	NIR minimum (reflectance)	S:N ratio	Field AT05 biomass	Field PC789 biomass	R^2
Measured				42833 ± 8175	43986 ± 8800	
SPOT 5	September 23	0.4432	38.2	60286 ± 6130	50853 ± 9578	0.19
SPOT 5	August 13	0.5200	71.9	45219 ± 5163	43669 ± 1250	0.36
SPOT 5	July 18	0.5200	57.8	42293 ± 5582	51581 ± 3754	0.36
Ikonos 2	September 07	0.4905	34.6	46879 ± 2487	33571 ± 1244	0.02
Ikonos 2	August 08	0.5160	36.4	32399 ± 4425	45231 ± 990	0.35
Quick-Bird 2	July 28	0.5157	39.2	–	44322 ± 1648	0.35
Landsat 5	August 16	0.5200	50.4	39284 ± 6260	43924 ± 1475	0.37

Table 6
Average spectral model estimates ± 1 standard deviation using satellite imagery for leaf quality (C:N ratio) and N content (%) by variety

Leaf	Date acquired 2003	Signal:noise	Sensor	R^2	ACS 999	Beta 6600	Holly 811	VDH 556
C:N	Measured				17.29 ± 3.02	12.82 ± 0.53	12.00 ± 1.63	12.88 ± 3.42
	September 7	15.8 Blue 25.6 Green	Ikonos	0.51	13.57 ± 0.10	13.42 ± 0.53	13.45 ± 0.21	13.21 ± 0.28
	September 23	59.1 Green	SPOT	0.36	15.88 ± 0.82	16.17 ± 0.46	16.48 ± 0.55	16.18 ± 0.57
N	Measured				2.73 ± 1.03	3.13 ± 0.19	3.27 ± 0.41	3.24 ± 0.93
	September 7	15.8 Blue 25.6 Green	Ikonos	0.55	2.94 ± 0.11	2.98 ± 0.11	2.97 ± 0.06	3.04 ± 0.06
	September 23	59.1 Green	SPOT	0.36	2.5 ± 0.23	2.42 ± 0.11	2.33 ± 0.15	2.42 ± 0.16

red bands would contribute to the model, we found that the NIR band alone provided the most accurate estimates.

3.2. Satellite application of ground-truth models

3.2.1. Canopy N and C:N ratio

Plant canopy N, computed by summing N mass for each leaf size group by plant, was similar among varieties, with an overall average of 30 mg g^{-1} dw. The ACS 999 variety contained a greater proportion of large leaves with significantly greater C:N ratio; consequently, ACS 999 mean canopy C:N ratio was greater than average leaf C:N ratio (Table 4). Plant canopy N and C:N ratios tend to change from the beginning to the end of the growing season as carbohydrates and nutrients are re-translocated below-ground. Therefore, most accurate spectral estimates

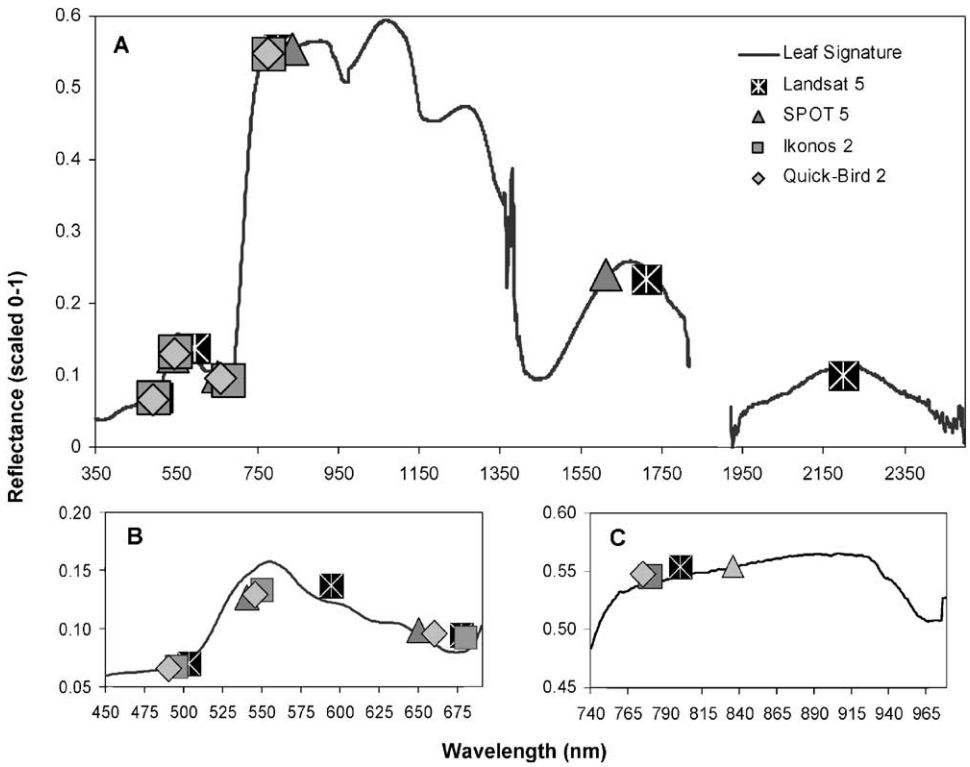

Fig. 5. Sugar beet leaf spectra (350–2500 nm), with enlargements of visible (B) and NIR (C) spectral regions highlighting center point differences among satellite sensors.

for potential aboveground residual C and N are near harvest at the end of September. Two images met these criteria, since they were acquired prior to harvest (SPOT 5 and Ikonos 2 sensors) and within 1 week of leaf chemical processing (Table 1).

SPOT 5 model estimates for canopy N and C:N ratio were significantly different from ground-truth data, according to a paired *t*-test comparison ($P < 0.05$). The SPOT 5 model tended to overestimate canopy C:N ratio and underestimate N (Table 6). Model errors were likely due to a combination of factors, including the lack of blue spectra, low predictive value of the formula ($r^2 = 0.36$), insufficient signal to noise ratio (S:N), and multi-spectral sensor peak offset (Fig. 5). Peak offset refers to the differences in the center point of the green band among sensors. The center of the SPOT green peak is 540 nm, which is shifted away from the narrow leaf signature peak of 550 nm. Offset error for this sharp peak of interest may skew model estimates toward higher C:N ratio and leaf N content, as found in our evaluation.

Ikonos 2 canopy N and C:N ratio estimates, however, were similar to leaf chemistry (Table 6), although estimates failed to detect the full range of measured variability among varieties. Error in the model formula ($r^2 = 0.51$) and low S:N ratios likely subsumed subtle differences between ACS 999 and

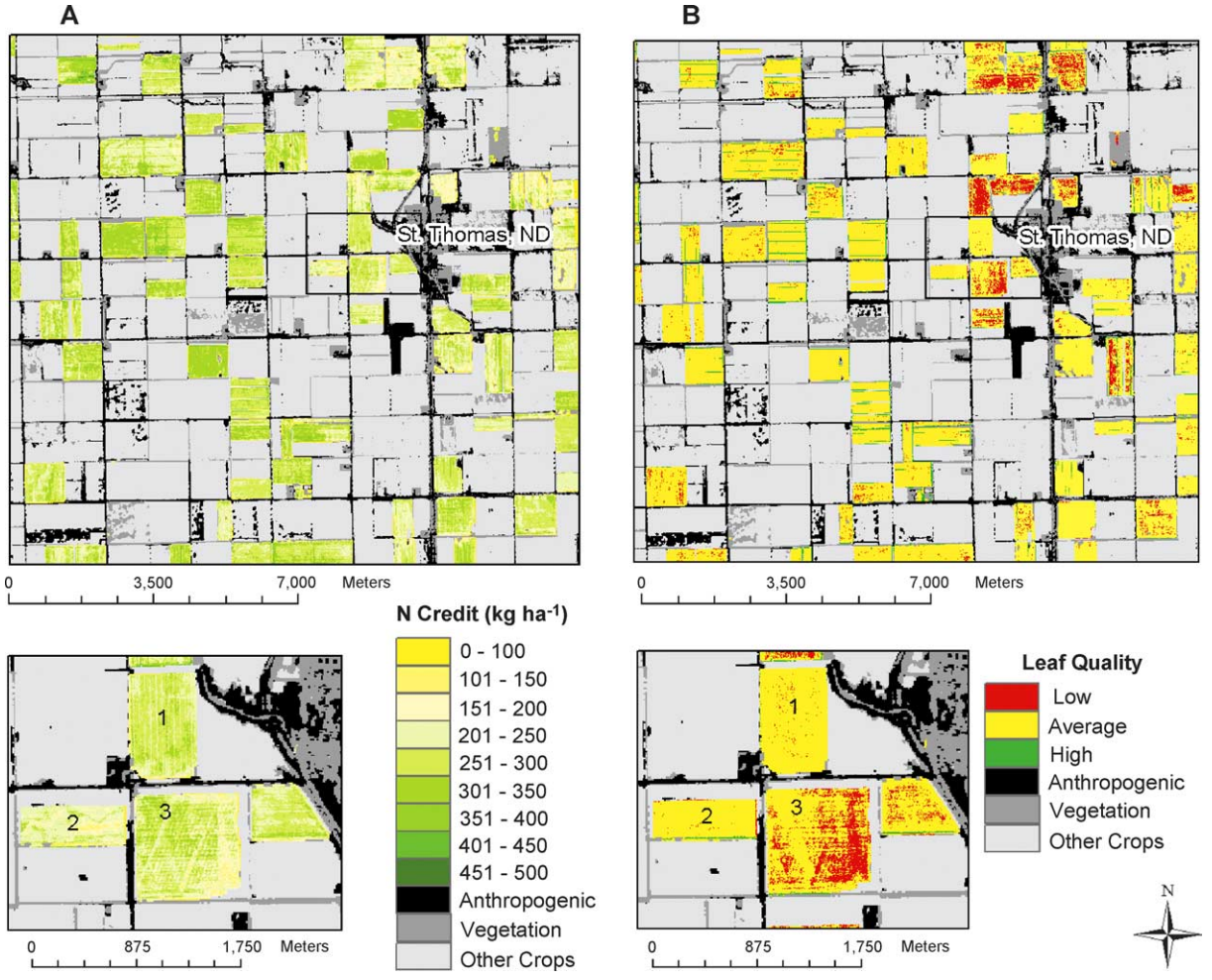

Fig. 6. N-credit and leaf quality maps with enlargements indicating sugar beet fields where C:N ratio is unusually high.

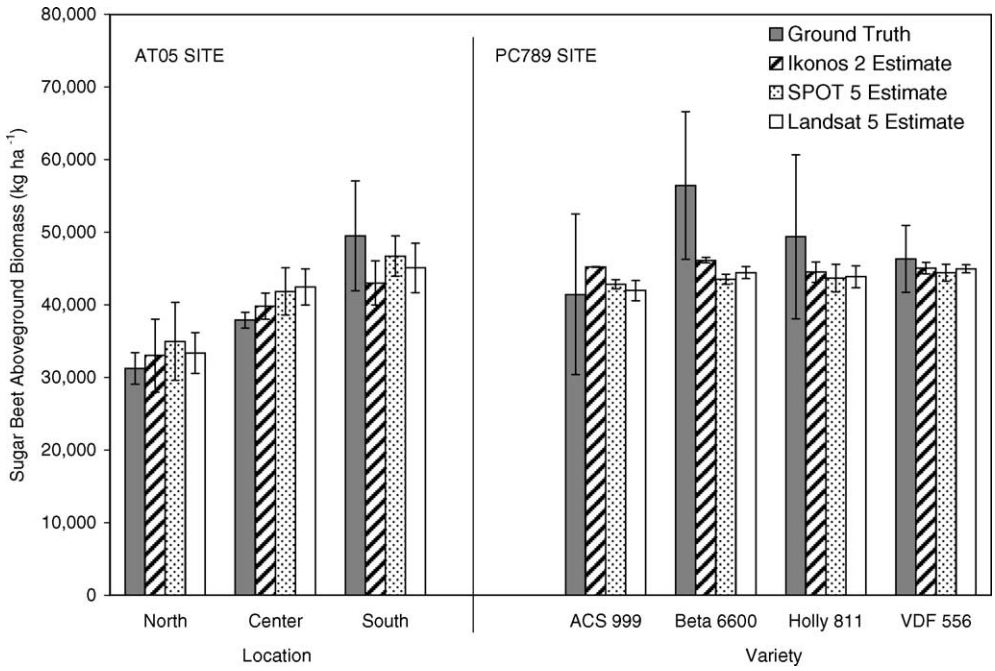

Fig. 7. Measured vs. satellite estimates (mean ± 1 standard deviation) for PC789 ($n = 15$) and AT05 ($n = 9$) biomass according to Ikonos 2, SPOT 5, and Landsat 5 data acquired in August.

Beta 6600 varieties. Our sugar beet leaf and canopy N measurements are representative of cultivated sugar beet leaves (Franzen et al., 2001), but satellite delineation within the measured range (25–45 mg g^{-1}) is not likely. Alternatively, we delineate areas where leaf tissue is unusually nutrient deficient or lower in quality using C:N ratio (Fig. 6). Aberrant leaf quality may be attributed to climate, weed invasions, plant pathogens, or other stress factors. Ultimately, N-credit for weedy or stressed sites should be evaluated as distinct from typical leaf residue sites.

3.2.2. Biomass

Sugar beet canopy NIR reflectance data were highly correlated (0.6–0.8) with biomass for highly productive beets with leaves at full canopy (Fig. 3), as demonstrated previously (Richardson and Wiegard, 1977; Jensen et al., 1998; Guerif and Duke, 2000; Boegh et al., 2002). Sugar beet canopy LAI can be estimated more accurately using the NIR band than the red or the green spectral bands (Guerif and Duke, 2000), due in part to the wide NIR plateau that minimizes formulae error and sensor-specific sensitivity (Fig. 5). In general, spatial variability within fields was subsumed by spectral model estimates (Table 5), but errors for August predictions were within 10–20% of measured biomass (see RMSE Table 3). In spite of errors introduced by the S:N ratio, sensor spatial resolution, and gradients in crop productivity, model estimates for August biomass using Ikonos 2, SPOT 5 and Landsat 5 were 84, 94, and 94% of the measured mean values, respectively (Table 5). Landsat 5 spatial resolution is coarser than Ikonos 2 and SPOT 5, but the S:N ratio is much greater. Consequently, the accuracy of biomass estimates using Landsat 5 is comparable to Ikonos 2 and SPOT 5 (Fig. 7).

3.2.3. N-credit satellite model

Canopies high in biomass and high in leaf N content could contribute enough soil N to mitigate fertilization the following year without impacting yield (Sims et al., 2002), and current multi-spectral sensor data can assist growers with canopy N content assessment. Sugar beet N-credit mapping is possible using multi-spectral satellites by coupling two

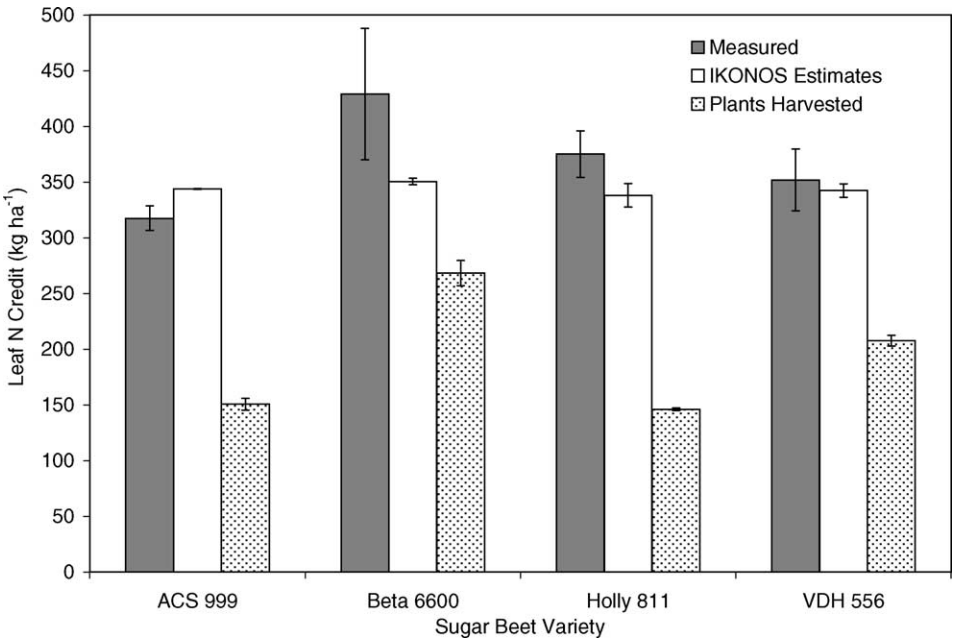

Fig. 8. Comparison of mean values (±1 standard deviation) calculated for N-credit using: (1) measured data (leaf biomass multiplied by leaf N content), (2) Ikonos spectral model estimates, and (3) harvest data (number of plants harvested multiplied by leaf N content).

formulae: (1) the quantitative spectral biomass formula and (2) the qualitative N formula that delineates average from low leaf N (Fig. 6A). Map results indicate variability within and between fields, ranging from ∼150 to 350 kg ha^{-1}. Leaf quality (high C:N ratio), on the other hand, may also be mapped to provide information that may help managers discern leaf quality from biomass or other issues (Fig. 6B). Spectral errors in the C:N ratio and leaf N models prevented quantitative leaf quality detection, however qualitative evaluation is feasible. Fig. 6B enlargement depicts fields (1 and 2) with average leaf quality; however, when compared with Fig. 6A, N-credit is lower for field 2. There may be other issues here that influence N-credit aside from leaf quality. Alternatively, leaf quality for field 3 is lower on the east side, which corresponds to lower N-credit. These high C:N ratio zones indicate potential differences in N mineralization rate, which will likely alter N-credit and N fertilization for these areas.

Satellite models tend to under-estimate N-credit, but they more closely resemble ground-truth data than N-credit calculated according to the number of plants harvested (Fig. 8). For this study, we calculated average N-credit for field PC789 according to ground data (∼350 kg ha^{-1}), Ikonos 2 (∼300 kg ha^{-1}) and number of plants harvested (∼200 kg ha^{-1}).

4. Discussion

Sugar beet residue contributes to the pool of potentially available N the following spring and reduces fertilizer requirements (Moraghan and Smith, 1996), and few spectral models applicable to leaf N detection have been created and evaluated using current satellite imagery. Previous studies conclude that the 550 and 700 nm (green and far-red) wavelengths are linearly related to the amount of leaf chlorophyll (Gitelson and Merzlyak, 1997), which is a nitrogenous molecule, but delineation for fresh leaf N is rarely tested on available multi-spectral imagery. Nitrogen in dry, ground plant material can be detected with ∼2100 nm spectra, but plant moisture obviates detection at this wavelength in natural ecosystems (Kokaly and Clark, 1999; Kokaly, 2001). Furthermore, chemical compounds (e.g., pigments) that share similar molecular structures

often overlap and interfere with spectral delineation (Curran et al., 1992). These factors, along with sensor sensitivity, contribute substantial error to satellite leaf N detection models.

The S:N ratio required for SPOT 5 and Ikonos 2 leaf N and C:N ratio detection were considerably lower than the recommended S:N ratio (Kokaly and Clark, 1999), which likely contributed to the problem of fine scale delineation of N and C:N ratio at the satellite level (Table 6). Actual S:N ratio in the NIR for biomass models varied among sensors (Table 5), although the NIR S:N ratio contributed less error to the biomass estimates than the visible bands. The N-credit model, then, depends upon sensor-specific S:N ratio that may be a substantive determinant to model reliability.

The NIR band represented biomass for these homogenous sugar beet agroecosystems at full cover using calibrated imagery, but this is contrary to researchers who recommend use of spectral ratios for biomass, such as NDVI or GNDVI. This index approach is particularly useful for minimizing differences in atmospheric and solar conditions between images and between vegetation species. In our case, minimizing image and vegetation variability was not necessary. For one, images were calibrated and errors for each band were identified so that derived formulae could be adjusted accordingly. Secondly, we are working with a monoculture where band combinations are not needed to represent a wide range of plant leaf thicknesses, pigments, etc. (Gitelson and Merzlyak, 1997). Instead of using established indices, we created ground-based models to estimate actual biomass using the NIR, and we did not find that NDVI or GNDVI improved accuracy (Senay et al., 2000; Boegh et al., 2002). For the purpose of N-credit estimation and separation of biomass from leaf N and C:N ratio, our results suggest application of NIR formulae for biomass estimation when utilizing calibrated imagery in homogenous agroecosystems.

5. Conclusion

Leaf level analyses indicated optimum N and C:N ratio detection in the green and blue spectral regions; however, convolved spectral data models applied to satellite imagery only marginally delineated leaf N and C:N. Satellite model estimates for leaf N and C:N were centered near the median, so only average and low leaf N content and C:N ratio could be estimated spectrally. This is likely due to the narrow green peak of interest, high S:N requirements, and peak offsets among satellite sensors. However, spectral estimates provided qualitative canopy assessment. Leaf C:N ratio models delineated areas of very poor leaf quality, such as weedy or stressed zones, that would potentially influence N availability the following year. Results represent the end of the 2003 season only, so additional leaf C and N measurements in subsequent years are advised to confirm that leaf material is within the range reported here.

Satellite N-credit models require specific acquisition times for leaf quality and biomass, and only two sensors (Ikonos 2 and SPOT 5) were available at both times for N-credit model evaluation. SPOT 5 lacks the spectral resolution required for leaf N detection, while Ikonos 2 spectral resolution was sufficient for predicting residual N to within 7% of actual measured N-credit (Fig. 8). Incorporated in these estimates are errors associated with senor spectral and spatial resolution, which subsume spatial variability in the 200–400 kg ha^{-1} range (Fig. 6), but aberrant zones of low or high leaf residue N are delineated. Despite issues with resolution, our spectral N-credit model depicted within-field variability with greater accuracy than the conventional method of multiplying the number of plants harvested by plant leaf N (Fig. 8).

Although further validation is recommended, the models described here demonstrate that satellite sensor data can be applied in agro-ecosystems to assist with N management. Aboveground sugar beet biomass and leaf quality may be estimated using satellite data when plants are at full cover and the NIR is >0.5, but spectral resolution offsets and optical errors hinder accuracy and must be taken into account. Each satellite sensor is spectrally unique; especially in the green, so N detection capability varies with sensor and detection limits may exceed detection of variability within a field. Nevertheless, derived sensor-specific models can estimate N-credit for agro-ecosystems, and the C:N ratio model can be applied to map aberrant leaf quality areas. Satellite N-credit estimation is particularly applicable for precision agriculture management, as this method can point to

variability within and between fields on a pixel-by-pixel basis. In summary, we evaluated the potential utility of multi-spectral N-credit estimations using four different satellite sensors for sugar beet growers who wish to avoid the economic and environmental impacts of over-fertilization.

Acknowledgements

We would like to acknowledge the USDA support for this project through Cooperative Agreement No. 58-5445-3-314; Edward Wene, University of Minnesota Crookston Agricultural Utilization Research Institute for laboratory equipment, and University of North Dakota's Bob Sherman (Biology Department), Assefa Melesse, Robert Fergeson, Steve Moe, Scott Bylin, and Juan Pedraza for lab and field assistance.

References

Abshahi, A., Hill, F.J., Broadbent, F.E., 1984. Nitrogen utilization by wheat from residual sugar beet fertilizer and soil incorporated sugar beet tops. Agron. J. 76, 954–958.

Boegh, E., Soegaard, H., Broge, N., Hasager, C.B., Jensen, N.O., Schelde, K., Thomsen, A., 2002. Airborne multispectral data for quantifying leaf area index, nitrogen concentration, and photosynthetic efficiency in agriculture. Remote Sens. Environ. 81, 179–193.

Bouman, B.A.M., 1992. Linking physical remote sensing models with crop growth simulation models, applied for sugar beet. Int. J. Remote Sens. 13, 2565–2581.

Chavez, P.S., 1996. Image-based atmospheric correction – revised and improved. Photogramm. Eng. Remote Sens. 62, 1025–1036.

Clevers, J.G.P.W., 1997. A simplified approach for yield prediction of sugar beet based on optical remote sensing data. Remote Sens. Environ. 61, 211–228.

Curran, P.J., Dungan, J.L., Macler, B.A., Plummer, E.S., Peterson, D.L., 1992. Reflectance spectroscopy of fresh whole leaves for the estimation of chemical concentration. Remote Sens. Environ. 39, 153–166.

Franzen, D.W., Giles, J.F., Reitmeier, L.J., Hapka, A.J., Hapka, A.J., Cattanach, N.R., Cattanach, A.C., 2001. Summary of four years of research on poor quality sugarbeets in a sugarbeet, spring wheat, potato rotation. Sugar Beet Res. Extension Rep. 32, 152–173.

Gitelson, A.A., Merzlyak, M.N., 1997. Remote estimation of chlorophyll content in higher plant leaves. Int. J. Remote Sens. 18, 2691–2697.

Guerif, M., Duke, C., 2000. Adjustment procedures of a crop model to the site specific characteristics of soil and crop using remote sensing data assimilation.. Agric. Ecosyst. Environ. 81, 57–69.

Huang, C., Zhang, Z., Yang, L., Wylie, B., Homer, C., 2002. MRLC 2000 Image Preprocessing Procedure. USGS White Paper.

Jacquemoud, S., Verdebout, J., Schmuck, G., Andreoli, G., Hosgood, B., 1995. Investigation of leaf biochemistry by statistics. Int. J. Remote Sens. 54, 180–188.

Jensen, J.R., Coombs, C., Porter, D., Jones, B., Schill, S.D.W., 1998. Extraction of smooth cord grass (*Spartina alterniflora*) biomass and leaf area index parameters from high resolution imagery. Ceocarto Int. 13, 25–34.

Kokaly, R.F., 2001. Investigating a physical basis for spectroscopic estimates of leaf nitrogen concentration. Remote Sens. Environ. 75, 153–161.

Kokaly, R.F., Clark, R.N., 1999. Spectroscopic determination of leaf biochemistry using band depth analysis of absorption features and stepwise linear regression. Remote Sens. Environ. 67, 267–287.

Leff, B., Ramankutty, N., Foley, J.A., 2004. Geographic distribution of major crops across the world. Global Biogeochem. Cycles 18, 1–27.

Moraghan, J.T., Smith, L.J., 1996. Nitrogen in sugarbeet tops and the growth of a subsequent wheat crop. Agron. J. 88, 521–526.

Moran, M.S., Inoue, Y., Barnes, E.M., 1997. Opportunities and limitations for image-based remote sensing in precision crop management. Remote Sens. Environ. 61, 319–346.

Mutanga, O., Skidmore, A.K., Prins, H.H.T., 2004. Predicting in situ pasture quality in the Kruger National Park, South Africa, using continuum-removed absorption features. Remote Sens. Environ. 89, 393–408.

NASA, 2003. Landsat-7 Science Data Users Handbook. Landsat Project Science Office, NASA Goddard Space Flight Center, Greenbelt, MD.

Nosengo, N., 2003. Fertilized to death. Nature 425, 894–895.

Reeves, M.C., Winslow, J.C., Running, S.W., 2001. Mapping weekly rangeland vegetation productivity using MODIS algorithms. J. Range Manage. 54, 90–105.

Richardson, A.J., Wiegard, C.L., 1977. Distinguishing vegetation from soil background information. PE & RS 43, 1541–1552.

Senay, G.B., Lyon, J.G., Ward, A.D., Nokes, S.E., 2000. Using high spatial resolution multispectral data to classify corn and soybean crops. Photometric Eng. Remote Sens. 66, 319–327.

Sims, A.L., Moraghan, J.T., Smith, L.J., 2002. Spring wheat response to fertilizer nitrogen following a sugar beet crop varying in canopy color. Precision Agric. 3, 283–295.

Vitousek, P.M., 1997. Human domination of Earth's ecosystems. Science 275, 494–501.

Vos, J., van der Putten, P.E.L., 2000. Nutrient cycling in a cropping system with potato, spring wheat, sugar beet, oats and nitrogen catch crops I. Input and offtake of nitrogen, phosphorus and potassium. Nutrient Cycling Agroecosyst. 56, 87–97.

Whitmore, A.P., Groot, J.J.R., 1997. The decomposition of sugar beet residues: mineralization versus immobilization in contrasting soil types. Plant Soil 192, 237–247.